High-order FEMs for thermo-hyperelasticity at finite strains

Zohar Yosibash, Danny Weiss
Computational Mechanics Lab., Dept. of Mechanical Engineering
Ben-Gurion University of the Negev, Beer-Sheva, Israel

Stefan Hartmann
Institute of Applied Mechanics
Clausthal University of Technology, Clausthal-Zellerfeld, Germany

Abstract

Thermo-hyperelastic problems at finite strains belong to a category of non-linear coupled problems that impose challenges on their numerical treatment. We present the weak-form for a 1-D coupled, stationary, thermo-hyperelastic system with constant or temperature-dependent material properties. The coupled system is discretized by a 'monolithic' high-order finite element method (p-FEM) based on hierarchical shape-functions. To verify the accuracy and to investigate the convergence rates of the p-FEM for the non-linear coupled problem, exact solutions are derived that are compared to the numerical results. These demonstrate the accuracy and efficiency of the applied p-FEMs.

1 Introduction

Coupled thermo-mechanical problems that undergo finite deformations with material properties that depend on the temperature field are of interest in many engineering applications. Such problems impose difficulties on their numerical treatment, part of which were investigated by classical finite element methods (FEMs) in the past, see e.g. Armero and Simo (1992). Here we apply high-order finite elements with hierarchical shape-functions based on integrated Legendre polynomials, constrain the problem to a one-dimensional setting, and consider the steady-state thermo-hyperelastic problem in a bar. This problem is described by two non-linear ordinary differential equations (ODEs) that are two-way coupled: the temperature field results in volumetric expansion and affects the mechanical properties as well as the heat conductivity, whereas the heat conduction equation has to be satisfied on a domain that deforms due to the mechanical loads and displacements. The 1-D problem is a typical example that is simple enough to enable exact solutions to be derived against which numerical solutions can be compared to demonstrate the convergence and accuracy properties.

The p-version of the FEMs has been successfully applied to non-linear mechanical problems of isotropic hyperelasticity in Düster et al. (2003); Heisserer et al. (2008); Yosibash et al. (2007); Netz et al. (2013), for anisotropy in Yosibash and Priel (2011) and the weakly and strongly coupled thermo-mechanical system was recently addressed in Erbts and Düster (2012). To the best of our knowledge this is the first

monolithic [1] implementation of p-FEMs to a coupled nonlinear thermo-mechanical system where the numerical results are evaluated against exact solutions (regular as well as singular ones) so that the accuracy and robustness can be assessed.

Notations and weak formulation, first of the solid mechanics part followed by the coupled thermo-mechanical system, are provided in section 2. In this section we also derive exact solutions against which the numerical results may be assessed for accuracy and efficiency. The linearization of the weak-form and the p-FE discretization are detailed in section 3. We then present p-FE results compared to the exact solutions in section 4 that demonstrate the accuracy and rates of convergence of the proposed p-FEMs.

2 Notations, preliminaries and 1-D formulation

To derive the one-dimensional test case, we consider the three-dimensional kinematical relations, the constitutive equations and the local balance equations for momentum and energy and subject them to the 1-D case with laterally constrained displacements and adiabatic boundary conditions. Consider a domain denoted by Ω_0 made of a hyperelastic material that is subjected to a temperature change $\Theta(\boldsymbol{X})$ and to mechanical loading. The mathematical model that governs the steady-state thermo-hyperelastic response in a 3-D domain consists of three nonlinear equilibrium equations in terms of the displacements in addition to a heat conduction equation, that are fully coupled. The coupling is manifested in the deformation gradient that is composed of mechanical and thermal parts, in the mechanical material properties that depend on the temperature, and because the heat conduction equation is to be solved on a domain that deforms depending on the displacements. Starting with the problem formulation in a 3-D setting, we reduce it in this section to a simplified 1-D case so that the axial displacement $U(X)$ and the temperature $\Theta(X)$ are governed by two coupled non-linear equations. This problem allows us to derive a set of exact solutions to be used as benchmark problems for verifying finite element schemes.

We denote the location of a material point in the undeformed configuration by $\boldsymbol{X}$ and its corresponding location in the deformed configuration Ω by $\boldsymbol{x}(\boldsymbol{X})$. The displacement vector is therefore $\boldsymbol{U}(\boldsymbol{X}) = \boldsymbol{x}(\boldsymbol{X}) - \boldsymbol{X}$. The deformation gradient is denoted by

$$\boldsymbol{F} = \text{Grad}\ \boldsymbol{x}, \rightarrow F_{ij} = \frac{\partial x_i}{\partial X_j} = \delta_{ij} + \frac{\partial U_i}{\partial X_j}.$$

In the following we introduce $J \overset{\text{def}}{=} \det \boldsymbol{F}$ describing the local volumetric deformation.

According to Lu and Pister (1975) the deformation gradient can be multiplicatively decomposed into a mechanical and a thermal part, $\boldsymbol{F} = \boldsymbol{F}_M \boldsymbol{F}_\Theta$. Alternatively, the decomposition $\boldsymbol{F} = \boldsymbol{F}_\Theta \boldsymbol{F}_M$ can be done leading to the same results in thermo-

[1] Monolithic is an accepted terminology to a fully coupled approach when equations are discretised and solved simultaneously.

hyperelasticity if a pure volumetrically thermal expansion is assumed, see Hartmann (2012).

The deformation gradient associated with temperature change is

$$\boldsymbol{F}_\Theta = \varphi \boldsymbol{I} \tag{1}$$

with

$$\varphi \stackrel{\text{def}}{=} 1 + \alpha_\Theta(\Theta - \Theta_0)$$

where α_Θ is the *thermal expansion coefficient* and Θ_0 is a reference temperature. This results in a pure volumetric deformation

$$J_\Theta \stackrel{\text{def}}{=} \det(\boldsymbol{F}_\Theta) = \varphi^3 = (1 + \alpha_\Theta(\Theta - \Theta_0))^3 . \tag{2}$$

This is the expected outcome of heating, which reduces to the well-known expression in small strain, linear thermo-elasticity at the limit.

The mechanical part of the volumetric deformation is $J_M = \det(\boldsymbol{F}_M)$, which can be determined by the total deformation and the temperature

$$\begin{gathered} J = \det(\boldsymbol{F}) = \det(\boldsymbol{F}_\Theta \boldsymbol{F}_M) = \det(\boldsymbol{F}_\Theta)\det(\boldsymbol{F}_M) = (1 + \alpha_\Theta(\Theta - \Theta_0))^3 J_M \\ \Downarrow \\ J_M = \frac{J}{\varphi^3} = \frac{J}{(1 + \alpha_\Theta(\Theta - \Theta_0))^3} \end{gathered} \tag{3}$$

that will be used in the definition of the specific free-energy.

Additionally, the right Cauchy-Green tensors

$$\boldsymbol{C} = \boldsymbol{F}^T \boldsymbol{F}, \qquad \boldsymbol{C}_M = \boldsymbol{F}_M^T \boldsymbol{F}_M, \tag{4}$$

are defined, where, in the following, the unimodular right Cauchy-Green tensors

$$\bar{\boldsymbol{C}} \stackrel{\text{def}}{=} (\det \boldsymbol{C})^{-1/3} \boldsymbol{C}, \quad \rightarrow \quad \det \bar{\boldsymbol{C}} = 1 \tag{5}$$

$$\bar{\boldsymbol{C}}_M \stackrel{\text{def}}{=} (\det \boldsymbol{C}_M)^{-1/3} \boldsymbol{C}_M, \quad \rightarrow \quad \det \bar{\boldsymbol{C}}_M = 1. \tag{6}$$

are required. One observes by simple mathematical evaluation that $\bar{\boldsymbol{C}}_M = \bar{\boldsymbol{C}}$ (see also Hartmann (2012)), and accordingly, $I_{\bar{\boldsymbol{C}}_M} = I_{\bar{\boldsymbol{C}}}$ hold.

On the basis of these deformation measures the specific free-energy

$$\rho_R \psi(\boldsymbol{C}_M, \Theta) = \rho_R \psi_{vol}(J_M) + \rho_R \psi_{iso}(I_{\bar{\boldsymbol{C}}_M}) + \rho_R \psi_\Theta(\Theta) \tag{7}$$

is assumed, where we have $\rho_R \psi_{iso}(I_{\bar{\boldsymbol{C}}}) = \rho_R \psi_{iso}(I_{\bar{\boldsymbol{C}}_M})$. According to Hartmann and Neff (2003) the volumetric part reads

$$\rho_R \psi_{vol}(J_M) = \frac{\kappa}{50} \left(J_M^5 + J_M^{-5} - 2 \right), \tag{8}$$

which does not lead to physically unlikely results in uniaxial compression and tension in a huge range of deformation, see Ehlers and Eipper (1998) for the underlying problem as well. For the isochoric part the Neo-Hookean model is assumed

$$\rho_R \psi_{iso}(I_{\bar{\boldsymbol{C}}}) = \rho_R \psi_{iso}(\mathrm{I}_{\boldsymbol{C}_M}, J_M) = c_{10}(\mathrm{I}_{\bar{\boldsymbol{C}}_M} - 3) = c_{10}(\mathrm{I}_{\boldsymbol{C}_M} J_M^{-2/3} - 3) \tag{9}$$

with c_{10} usually related to the shear modulus $\mu/2$ in the limit of the small strain case.

The expression of the 2^{nd} Piola-Kirchhoff stress tensor

$$\tilde{\boldsymbol{T}} = 2\rho_R \frac{\partial \psi(\boldsymbol{C}, \Theta)}{\partial \boldsymbol{C}} \tag{10}$$

can be computed by the stress tensor $\hat{\boldsymbol{S}}$ *relative to the thermal intermediate configuration*

$$\hat{\boldsymbol{S}} = 2\rho_R \frac{\partial \psi}{\partial \boldsymbol{C}_M} = 2\rho_R \left(\frac{d\psi_{vol}}{dJ_M} \frac{\partial J_M}{\partial \boldsymbol{C}_M} + \frac{\partial \psi_{iso}}{\partial J_M} \frac{\partial J_M}{\partial \boldsymbol{C}_M} + \frac{\partial \psi_{iso}}{\partial \mathrm{I}_{\boldsymbol{C}_M}} \frac{\partial \mathrm{I}_{\boldsymbol{C}_M}}{\partial \boldsymbol{C}_M} \right), \tag{11}$$

where

$$\tilde{\boldsymbol{T}} = \boldsymbol{F}_\Theta^{-1} \hat{\boldsymbol{S}} \boldsymbol{F}_\Theta^{-T}. \tag{12}$$

In view of Eq.(11) the derivatives read

$$\begin{aligned} \rho_R \frac{d\psi_{vol}}{dJ_M} &= \frac{\kappa}{10} \left(J_M^4 + J_M^{-6} \right) \\ \rho_R \frac{\partial \psi_{iso}}{\partial J_M} &= \frac{-2c_{10}}{3} \mathrm{I}_{\boldsymbol{C}_M} J_M^{-5/3} \\ \rho_R \frac{\partial \psi_{iso}}{\partial \mathrm{I}_{\boldsymbol{C}_M}} &= c_{10} J_M^{-2/3} \end{aligned} \tag{13}$$

The calculation of $\partial J_M / \partial \boldsymbol{C}_M$ is performed similarly to $\partial \mathrm{III}_{\boldsymbol{C}} / \partial \boldsymbol{C} = \mathrm{III}_{\boldsymbol{C}} \boldsymbol{C}^{-1}$. First we evaluate

$$\frac{\partial \mathrm{III}_{\boldsymbol{C}M}}{\partial \boldsymbol{C}_M} = \mathrm{III}_{\boldsymbol{C}M} \boldsymbol{C}_M^{-1} \tag{14}$$

On the other hand

$$\mathrm{III}_{\boldsymbol{C}M} = J_M^2, \quad \rightarrow \frac{\partial \mathrm{III}_{\boldsymbol{C}M}}{\partial \boldsymbol{C}_M} = 2J_M \frac{\partial J_M}{\partial \boldsymbol{C}_M}, \quad \rightarrow \frac{\partial J_M}{\partial \boldsymbol{C}_M} = \frac{1}{2J_M} \frac{\partial \mathrm{III}_{\boldsymbol{C}M}}{\partial \boldsymbol{C}_M} \tag{15}$$

holds. Substituting (14) in (15) leads to

$$\frac{\partial J_M}{\partial \boldsymbol{C}_M} = \frac{1}{2J_M} \mathrm{III}_{\boldsymbol{C}M} \boldsymbol{C}_M^{-1} = \frac{1}{2} J_M \boldsymbol{C}_M^{-1}. \tag{16}$$

Analogously to $\partial \mathrm{I}_{\boldsymbol{C}} / \partial \boldsymbol{C} = \boldsymbol{I}$ we calculate

$$\frac{\partial \mathrm{I}_{\boldsymbol{C}_M}}{\partial \boldsymbol{C}_M} = \boldsymbol{I}. \tag{17}$$

In conclusion, the substitution of (13), (16) and (17) into (11) yields

$$\hat{\boldsymbol{S}} = \frac{\kappa}{10} \left(J_M^5 + J_M^{-5} \right) \boldsymbol{C}_M^{-1} + 2c_{10} J_M^{-2/3} \left[\boldsymbol{I} - \frac{1}{3} \mathrm{I}_{\boldsymbol{C}_M} \boldsymbol{C}_M^{-1} \right] \tag{18}$$

or by applying (12) the 2^{nd} Piola-Kirchhoff tensor reads

$$\tilde{\mathbf{T}} = \frac{\kappa}{10} \left(J_M^5 + J_M^{-5} \right) \boldsymbol{C}^{-1} + 2c_{10} J^{-2/3} \left[\boldsymbol{I} - \frac{1}{3} \mathrm{I}_{\boldsymbol{C}} \boldsymbol{C}^{-1} \right] \tag{19}$$

using Eq.(18) with J_M defined in (3).

Restriction to a 1-D problem

Consider a prismatic cylinder constrained in the transverse directions (Y and Z). Denote by $U(X)$ the displacement at location X, thus

$$x(X) = X + U(X) \;\rightarrow\; \frac{\partial x}{\partial X} = 1 + \frac{\partial U(X)}{\partial X} \equiv 1 + U',$$

where the prime indicates the derivative with respect to the axial coordinate X in the reference configuration, $U' = \frac{dU(X)}{dX}$. In the other two directions $z = Z$ and $y = Y$, leading to the deformation gradient

$$\boldsymbol{F} = \begin{bmatrix} 1+U' & 0 & 0 \\ 0 & 1 & 0 \\ 0 & 0 & 1 \end{bmatrix} \tag{20}$$

Following (20) one obtains

$$J = \det(\boldsymbol{F}) = 1 + U' \quad \Longrightarrow J_M = \frac{J}{\varphi^3} = \frac{1+U'}{\left[1 + \alpha_\Theta(\Theta - \Theta_0)\right]^3}, \tag{21}$$

$$\boldsymbol{C} = \boldsymbol{F}^T\boldsymbol{F} = \begin{bmatrix} (1+U')^2 & 0 & 0 \\ 0 & 1 & 0 \\ 0 & 0 & 1 \end{bmatrix} \Rightarrow \boldsymbol{C}^{-1} = \begin{bmatrix} \frac{1}{(1+U')^2} & 0 & 0 \\ 0 & 1 & 0 \\ 0 & 0 & 1 \end{bmatrix}, \tag{22}$$

and, furthermore,

$$\boldsymbol{C}_M = \varphi^{-2}\boldsymbol{C} \;\Rightarrow \mathrm{I}_{C_M} = \mathrm{tr}(\boldsymbol{C}_M) = \varphi^{-2}\mathrm{tr}(\boldsymbol{C}) = \varphi^{-2}\left(2 + (1+U')^2\right). \tag{23}$$

Substituting (22), (23) and (3) in (19) we can explicitly express the axial stresses

$$\tilde{T}_{XX} = \frac{\kappa}{10}\left[\frac{(1+U')^3}{\varphi^{15}} - \frac{\varphi^{15}}{(1+U')^7}\right] + \frac{4c_{10}}{3}(1+U')^{-2/3}\left[1 - \frac{1}{(1+U')^2}\right]. \tag{24}$$

2.1 1-D Weak Form of Mechanical Part

The derivation of the weak form includes one part that is associated with the body forces. Denoting by $\rho\boldsymbol{g}$ the force per unit of volume ($\boldsymbol{g}$ may be interpreted as the acceleration or as force per unit of mass in spatial configuration), then equilibrium equations in spatial configuration are

$$\mathrm{div}\boldsymbol{\sigma} + \rho\boldsymbol{g} = 0, \quad \text{in } \Omega,$$

where $\boldsymbol{\sigma} = J^{-1}\boldsymbol{F}\tilde{\boldsymbol{T}}\boldsymbol{F}^T$ is the Cauchy stress tensor. Multiplying the equilibrium equations by a test function $\boldsymbol{v}$ and integrating over the domain Ω, the weak form *associated with the body forces* is given by

$$\int_\Omega \rho\boldsymbol{g}(\boldsymbol{x}) \cdot \boldsymbol{v}(\boldsymbol{x}) d\Omega. \tag{25}$$

Expressing this in the reference configuration we make use of the connections

$$\Omega = J\Omega_0, \quad \rho = \rho_R/J, \quad \boldsymbol{G}(\boldsymbol{X}) = \boldsymbol{g}(\boldsymbol{x}(\boldsymbol{X})), \tag{26}$$

where $\rho_R\boldsymbol{G}$ is the force per unit of volume of the reference configuration. Thus, (25) becomes

$$\int_{\Omega_0} \rho_R \boldsymbol{G}(\boldsymbol{X}) \cdot \boldsymbol{V}(\boldsymbol{X}) d\Omega_0. \tag{27}$$

The stationary Total-Lagrange formulation in 3-D is given in general as

$$\begin{gathered} \text{Seek } \boldsymbol{U} \in \overset{\circ}{\boldsymbol{\mathcal{E}}}(\Omega_0) \text{ such that } \forall \boldsymbol{V} \in \overset{\circ}{\boldsymbol{\mathcal{E}}}(\Omega_0) \\ \underbrace{\int_{\Omega_0} \tilde{\mathbf{T}} : \boldsymbol{E}(\boldsymbol{V}) d\Omega_0}_{\mathcal{P}^{Int}(\boldsymbol{u},\boldsymbol{V})} - \underbrace{\left(\int_{\partial\Omega_{0T}} \left(\boldsymbol{T} \cdot \boldsymbol{N} \right) \cdot \boldsymbol{V} d\Gamma_0 + \int_{\Omega_0} \rho_R \boldsymbol{G} \cdot \boldsymbol{V} d\Omega_0 \right)}_{\mathcal{P}^{Ext}(\boldsymbol{u},\boldsymbol{V})} = 0 \end{gathered} \tag{28}$$

where

$$\boldsymbol{E}(\boldsymbol{V}) \overset{\text{def}}{=} \frac{1}{2} \left[(\nabla_0 \boldsymbol{V})^T \boldsymbol{F}(\boldsymbol{U}) + \boldsymbol{F}^T(\boldsymbol{U}) \nabla_0 \boldsymbol{V} \right] \tag{29}$$

defines the virtual strain tensor, with $\text{Grad}\boldsymbol{V} = (\nabla_0 \boldsymbol{V})$, $\boldsymbol{T}$ being the first Piola-Kirchhoff stress tensor ($\boldsymbol{T} = J\boldsymbol{\sigma}\boldsymbol{F}^{-T}$), and $\boldsymbol{N}$ being the normal to the boundary in the reference configuration. The space $\overset{\circ}{\boldsymbol{\mathcal{E}}}(\Omega_0)$ is defined according to (Le Tallec, 1994, (7.2) on p. 492):

$$\overset{\circ}{\boldsymbol{\mathcal{E}}}(\Omega_0) \overset{\text{def}}{=} \left\{ \boldsymbol{U} \in W^{1,s}(\Omega_0), \boldsymbol{U}\Big|_{\partial\Omega_{0U}} = \mathbf{0} \right\}$$

Where $W^{1,s}(\Omega_0)$ is the Sobolev space and the number s is such that the first integral in (28) makes sense for any choice of $\boldsymbol{U}$ and $\boldsymbol{V}$. $\partial\Omega_{0U}$ denotes the part of the reference configuration's boundary on which homogeneous displacement boundary conditions are applied.

Reducing (28) to the 1-D case, results in the following simplifications:

$$\boldsymbol{U} \to U(X), \quad \int_{\Omega_0} \to \int_{X_0}^{L}, \quad d\Omega_0 \to dX$$

$$\tilde{\mathbf{T}} : \boldsymbol{E}(\boldsymbol{V}) \to \tilde{T}_{XX}(U', \Theta, X) \frac{dV}{dX}(1 + U') = \tilde{T}_{XX}(U', \Theta, X) \frac{dV}{dX} J$$

Furthermore, since accelerations are negligible and that we clamp the specimen at $X = X_0$ and prescribe a given force $F_L = T_{Xx}A = F_{11}\tilde{T}_{XX}$ (assuming the area is 1) at $X = L$, (28) becomes

$$\begin{gathered} \text{Seek } U(X) \in \overset{\circ}{\mathcal{E}}(X_0, L) \text{ such that } \forall V(X) \in \overset{\circ}{\mathcal{E}}(X_0, L) \\ \int_{X_0}^{L} \tilde{T}_{XX}(U', \Theta, X) V' J \, dX - \int_{X_0}^{L} \rho_R G_X V dX - F_L V(L) = 0 \end{gathered} \tag{30}$$

Here $\overset{\circ}{\mathcal{E}}(X_0, L)$ is :

$$\overset{\circ}{\mathcal{E}}(X_0, L) \overset{\text{def}}{=} \left\{ U \in W^{1,s}(X_0, L), U\Big|_{\partial\Omega_{0U}} = 0 \right\}, \quad \Omega_0 \overset{\text{def}}{=} \{X_0 < X < L\}$$

Where s is such that the first integral in (30) makes sense for any choice of U and V.

2.2 Analytic Solutions to the Mechanical Part of the Thermo-Hyperelastic Problem

In the following the reference domain $\Omega_0 = \{X|1 < X < 2\ \}$ is assumed. In the first example, we consider a decoupled problem, i.e. $\varphi = 1$ and according to (21)

$$J = J_M = 1 + U', \quad \text{and also } F_{11} = 1 + U' \tag{31}$$

The material properties are taken to be

$$\kappa = 1/2, \quad c_{10} = 3/16.$$

These values are taken so that at the limit of small strain linear elasticity the Poisson ratio is within the limits 0 and 0.5. For the particular choice one obtains ($\mu = 2c_{10}$)

$$\nu = \frac{3\kappa - 2\mu}{6\kappa + 2\mu} = 0.2$$

To generate Neumann BCs at $X = 2$, one needs to use the constitutive equation to determine the stress by (24)

$$\tilde{T}_{XX} = \frac{\kappa}{10}\left[(1+U')^3 - (1+U')^{-7}\right] + \frac{4}{3}c_{10}(1+U')^{-2/3}\left[1 - (1+U')^{-2}\right] \tag{32}$$

A common scalar "measure" of the solution is the strain-energy $\mathcal{U}(\Omega_0)$ which may be computed for a given free-energy by

$$\mathcal{U}(\Omega_0) = \int_{X=1}^{X=2} (\rho_R\psi_{vol} + \rho_R\psi_{iso})\, dX. \tag{33}$$

2.2.1 An exact solution without body forces $U(X) = X - 1$

Consider the solution

$$U(X) = X - 1 \ \rightarrow\ U' = 1, \quad J = 2, \quad F_{11} = 2 \tag{34}$$

The boundary conditions associated with the analytical solution (34). At $X = 1$, by substitution, one obtains the Dirichlet boundary conditions (BC)

$$U(1) = 0 \tag{35}$$

If (34) is substituted in (32) one obtains

$$\tilde{T}_{XX} = 0.517726973428 \tag{36}$$

Having the 2^{nd} Piola-Kirchhoff stress, one may immediately compute the Cauchy stress:

$$\sigma_{xx} = \frac{1}{J}F_{11}\tilde{T}_{XX}F_{11} = 1.03545394686 \tag{37}$$

which is a constant stress at each point of the domain. Thus, it satisfies the equilibrium equation *without body forces* (homogeneous deformation and stress state).

For a cross section of 1, the force (Neumann BC) at the right end $X = 2$ is given by

$$F_L = F_{11}(X = 2)\tilde{T}_{XX}(X = 2) = 2 \times 0.517726973428 = 1.03545394686 \tag{38}$$

The strain energy for this case is computed by (33) and reads

$$\mathcal{U}(\Omega_0) = 0.446518090566. \tag{39}$$

2.2.2 An exact 1st solution $U(X) = X^2 - X$ that generates body forces

The solution is taken to be

$$U(X) = X^2 - X \qquad \rightarrow J = 1 + U' = 2X, \quad F_{11} = 2X \tag{40}$$

The Dirichlet boundary condition associated with the analytical solution (40) at $X = 1$ is defined by

$$U(1) = 0 \tag{41}$$

To generate Neumann BCs at $X = 2$, we first compute the 2^{nd} P-K stress using (32)

$$\begin{aligned} \tilde{T}_{XX} &= \frac{\kappa}{10}\left((2X)^3 - (2X)^{-7}\right) + \frac{4c_{10}}{3}(2X)^{-2/3}\left[1 - (2X)^{-2}\right] \\ &\Rightarrow \quad \tilde{T}_{XX}(X = 2) = 3.29300872863 \end{aligned} \tag{42}$$

For a cross section of 1, the force (Neumann BC) at the right end $X = 2$ is given by:

$$F_L = F_{11}(X = 2)\tilde{T}_{XX}(X = 2) = 4 \times 3.29300872863 = 13.1720349145 \tag{43}$$

For (40) to be the solution, it has to satisfy the equilibrium equation in the deformed configuration, i.e.

$$\frac{\partial \sigma_{xx}}{\partial x} + \rho g_x = 0, \tag{44}$$

The equilibrium equation can also be stated in the reference configuration:

$$\frac{1}{F_{11}}\frac{d(F_{11}\tilde{T}_{XX})}{dX} + \frac{1}{J}\rho_R G_X = 0, \quad X \in (1, 2) \tag{45}$$

If we choose to consider (44) we have $\boldsymbol{\sigma} = \frac{1}{J}\boldsymbol{F}\tilde{\boldsymbol{T}}\boldsymbol{F}^T$ which in 1-D turns into $\sigma_{xx} = \frac{1}{J}F_{11}\tilde{T}_{XX}F_{11}$. To compute ρg_x and from it $\rho_R G_X$, we proceed as follows:

$$\frac{\partial \sigma_{xx}}{\partial x} = \frac{d\sigma_{xx}}{dX}\frac{dX}{dx} = \frac{d(2X\tilde{T}_{XX})}{dX} \times \frac{1}{2X} = -\rho g_x \tag{46}$$

which yields:

$$\rho g_x = -\left\{\frac{\kappa}{10}\left[8(2X)^2 + 12(2X)^{-8}\right] + \frac{8c_{10}}{9}(2X)^{-2/3}\left(1 + 5(2X)^{-2}\right)\right\} \tag{47}$$

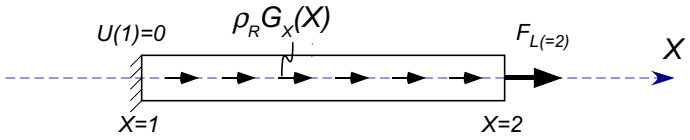

Figure 1: An illustration of the hyperelastic problem.

$$\rho_R G_X = J\rho g_x = -2X \times \left\{ \frac{\kappa}{10}\left[8(2X)^2 + 12(2X)^{-8}\right] + \frac{8c_{10}}{9}(2X)^{-2/3}\left(1 + 5(2X)^{-2}\right) \right\} \tag{48}$$

An illustrative example of the hyperelastic problem is depicted in Figure 1. Finally, the strain energy for this case is computed by (33)

$$\mathcal{U}(\Omega_0) = 3.779765536600198. \tag{49}$$

2.2.3 An exact 2nd solution $U(X) = X^3 - X$ that generates body forces

Next, the solution is taken to be

$$U(X) = X^3 - X, \quad \rightarrow J = F_{11} = 1 + U' = 3X^2 \tag{50}$$

The boundary conditions associated with the analytical solution (50) are computed similarly to (41) and (43)

$$\begin{aligned} U(1) &= 0 && (51)\\ F(2) &= F_{11}(X=2)\tilde{T}_{XX}(X=2) = && (52)\\ &= 12 \times \left\{ \frac{\kappa}{10}\left((12)^3 - (12)^{-7}\right) + \frac{4c_{10}}{3}(12)^{-2/3}\left[1 - (12)^{-2}\right] \right\} = 1037.3683824 \end{aligned}$$

and the body forces are:

$$\rho_R G_X = -3X^2 \times \left\{ \frac{\kappa}{10}\left[8(3X^2)^3 + 12(3X^2)^{-7}\right] + \frac{8c_{10}}{9}(3X^2)^{-2/3}\left(1 + 5(3X^2)^{-2}\right) \right\} \frac{1}{X} \tag{53}$$

The strain energy for this case is computed by (33)

$$\mathcal{U}(\Omega_0) = 454.3184883477279. \tag{54}$$

2.2.4 An exact 3rd solution $U(X) = X^4 - X$ that generates body forces

In the third example the solution is assumed to be

$$U(X) = X^4 - X, \quad \rightarrow J = F_{11} = 1 + U' = 4X^3 \tag{55}$$

According to the previous examples the boundary conditions associated with the analytical solution (55) are computed similarly to (41) and (43) first

$$U(1) = 0 \tag{56}$$

$$F(2) = F_{11}(X=2)\tilde{T}_{XX}(X=2) = 32 \times \left\{ \frac{\kappa}{10}\left((32)^3 - (32)^{-7}\right) + \frac{4c_{10}}{3}(32)^{-2/3}\left[1-(32)^{-2}\right] \right\}$$

$$= 52429.5929254 \tag{57}$$

yielding the body forces

$$\rho_R G_X = -4X^3 \times \left\{ \frac{\kappa}{10}\left[4(4X^3)^3 + 6(4X^3)^{-7}\right] + \frac{4c_{10}}{9}(4X^3)^{-2/3}\left(1+5(4X^3)^{-2}\right) \right\} \frac{3}{X} \tag{58}$$

Accordingly, the strain energy reads

$$\mathcal{U}(\Omega_0) = 41949.27332501347 \tag{59}$$

Remark 2.1 *Notice that the solution is such that at the end of the bar of length 1 we obtain a displacement of* $2^4 - 2 = 14$. *This results in an enormous stretch ratio.*

2.3 The Weak Form for the Heat-Conduction Part of the Thermo-Hyperelastic Problem

The point of departure is the weak formulation in current configuration, equation (33) in Hartmann et al. (2013):

$$-\int_\Omega c_{p_R}(\Theta)\dot{\Theta}\Upsilon d\Omega + \int_{\partial\Omega_N} q_n \Upsilon d\Gamma - \int_\Omega k_R(\nabla\Theta)\cdot(\nabla\Upsilon)d\Omega + \int_\Omega \rho(r-\gamma(\dot{\boldsymbol{E}},\Theta))\Upsilon d\Omega = 0 \tag{60}$$

Since we are interested in the steady-state solution, then the outmost left term of (60) is zero. We also assume quasi-static processes thus $\dot{\boldsymbol{E}} = \boldsymbol{0}$ so that (60) simplifies to

$$\int_{\partial\Omega_N} q_n \Upsilon d\Gamma - \int_\Omega k_R(\nabla\Theta)\cdot(\nabla\Upsilon)d\Omega + \int_\Omega \rho r \Upsilon d\Omega = 0 \tag{61}$$

To formulate (61) in reference configuration, we need to perform a pull-back operation. Since $d\Omega = Jd\Omega_0$, and in 1-D, $\nabla \to \frac{d}{dx}$, thus $\frac{d}{dx} = \frac{d}{dX}\frac{dX}{dx} = \frac{1}{F_{11}}\frac{d}{dX}$.

Similar to the treatment of the body forces in (25), $r(x)$ is the heat source per unit of mass and we have the following connections

$$\Omega = J\Omega_0, \quad \rho = \rho_R/J, \quad R(X) = r(x(X)) \tag{62}$$

where $\rho_R R(X)$ is the heat-source per unit of volume in the reference configuration. Consider Dirichlet boundary conditions $(\Theta - \Theta_0)\Big|_{X=X_0} = 0$, (61) becomes:

$$\text{Seek } \Theta(X) \in \overset{\text{o}}{\mathcal{E}}(X_0, L) \text{ such that } \forall \Upsilon(X) \in \overset{\text{o}}{\mathcal{E}}(X_0, L)$$

$$0 = -\int_{X_0}^{L} k_R \frac{\partial\Theta}{\partial X}\frac{\partial\Upsilon}{\partial X}\frac{1}{J}dX - k_R \frac{d\Theta(X)}{dX}\frac{1}{F_{11}}\Big|_{X=L}\Upsilon(L) - \int_{X_0}^{L}\rho_R R\Upsilon dX \tag{63}$$

In (63) we used the following notation

$$q_n \stackrel{\text{def}}{=} -k_R \frac{d\Theta}{dx} = -k_R \frac{d\Theta}{dX}\frac{dX}{dx} = -k_R \frac{d\Theta(X)}{dX}\frac{1}{F_{11}} \tag{64}$$

One may easily notice that (63) is linear in $\Theta(X)$ and the only non-linearity results from the coupling with U' through J. Here, we have assumed that Fourier's model has a constant heat conductivity in the material description, $k_R = \text{const}$.

2.4 The Coupled Thermo-Hyperelastic Weak Form in 1-D

Combining (30) and (63) we finally obtain the nonlinear coupled system to be solved

$$\text{Seek } (U(X), \Theta(X)) \in \overset{\circ}{\mathcal{E}}(X_0, L) \times \overset{\circ}{\mathcal{E}}(X_0, L) \text{ such that } \forall (V(X), \Upsilon(X)) \in \overset{\circ}{\mathcal{E}}(X_0, L) \times \overset{\circ}{\mathcal{E}}(X_0, L)$$

$$\int_{X_0}^{L} \tilde{T}_{XX}\, V' J\, dX - \int_{X_0}^{L} \rho_R G_X V dX - F_L V(L) = 0 \tag{65}$$

$$\int_{X_0}^{L} k_R\, \Theta'\, \Upsilon' \tfrac{1}{J}\, dX - \int_{X_0}^{L} \rho_R R dX - k_R \tfrac{d\Theta(X)}{dX}\tfrac{1}{F_{11}}\Big|_{X=L} \Upsilon(L) = 0 \tag{66}$$

To simplify notation, the nonlinear functionals (65) and (66) are denoted by

$$\mathcal{S}\Big(U(X), \Theta(X); V(X), \Upsilon(X)\Big) = 0 \tag{67}$$

$$\mathcal{T}\Big(U(X), \Theta(X); V(X), \Upsilon(X)\Big) = 0 \tag{68}$$

2.4.1 A solution to the coupled thermo-hyperelastic problem with constant coefficients

Consider the same 1-D bar and and material properties as in the previous examples with $\kappa = 1/2, \quad c_{10} = 3/16$. Additionally, the coefficient of thermal expansion is $\alpha_\Theta = 10^{-5}$ and the thermal conductivity is $k_R = 1$. The solution is taken to be

$$U(X) = X^2 - X \qquad \rightarrow J = 1 + U' = 2X, \quad F_{11} = 2X \tag{69}$$

$$\Theta(X) = X^2 - X \tag{70}$$

Since the temperature Θ is to be understood as the difference compared to a reference stress-free temperature, we choose the reference temperature $\Theta_0 = 0$.

The boundary conditions associated with the solution (69)-(70) at $X = 1$ are

$$U(1) = 0, \quad \Theta(1) = 0 \tag{71}$$

Two BCs are required at $X = 2$ for the coupled system. For the mechanical system one must first compute the 2^{nd} P-K stress using (24). For this purpose $\varphi = 1 + \alpha_\Theta(\Theta - \Theta_0) = 1 + \alpha_\Theta(X^2 - X)$, so that

$$\tilde{T}_{XX} = \frac{\kappa}{10}\left(\frac{(2X)^3}{(1+\alpha_\Theta(X^2-X))^{15}} - \frac{(1+\alpha_\Theta(X^2-X))^{15}}{(2X)^7}\right) + \frac{4c_{10}}{3}(2X)^{-2/3}\left[1 - (2X)^{-2}\right] \tag{72}$$

For a cross section of 1, the force at the right end $X = 2$ is given by:

$$F_L = F_{11}(X = 2)\tilde{T}_{XX}(X = 2) = 13.1681955252 \tag{73}$$

The flux BC at $X = 2$ is computed according to (64):

$$q_n(X = 2) = -k_R \frac{d\Theta(X)}{dX}\frac{1}{J} = -k_R \frac{2X-1}{2X}\bigg|_{X=2} = -k_R \frac{3}{4}$$

In addition to the BCs one has also to prescribe a body force and a distributed heat source so to obtain the required analytical solution. The body force is obtained by inserting (72) into (46), and using the relationship $\rho_R G_X = J\rho g_x$:

$$\rho_R G_X = 2X \times \left\{ \left[\frac{4X^2}{\varphi_1^{15}} - \frac{\varphi_1^{15}}{256X^8} \right] + \frac{\kappa}{10} G_2 - \frac{c_{10}}{9(2X)^{2/3}} \left(\frac{4}{X} + \frac{5}{X^3} \right) \right\} \tag{74}$$

with

$$\varphi_1 = -(1 + \alpha_\Theta(X^2 - X)),$$

$$G_2 = \frac{24X^2}{\varphi_1^{15}} + \frac{7\varphi_1^{15}}{128X^8} + \frac{128X^3\alpha_\Theta(2X-1)}{\varphi_1^{16}} + \frac{15\alpha_\Theta(2X-1)\varphi_1^{14}}{128X^7}.$$

The strong form of the heat equation in the deformed configuration is:

$$-\frac{dq}{dx} + \rho r(x) = 0.$$

For the particular case addressed herein we have $k_R = 1$ and

$$\frac{d}{dx} = \frac{1}{2X}\frac{d}{dX}.$$

Furthermore, the Fourier heat conduction $q = -k_R \frac{d\Theta}{dx}$ yields

$$\rho r(x) = -\frac{1}{4X^3} \tag{75}$$

Thus, similarly to the equilibrium equation we have:

$$\rho_R R(X) = J\rho r(x) = -2X \times \frac{1}{4X^3} = -\frac{1}{2X^2} \tag{76}$$

The heat equation can also be stated in the reference configuration where the coupling between the temperature and displacement is clearly stated:

$$\frac{1}{F_{11}}\frac{d}{dX}\left(k_R \frac{1}{F_{11}}\frac{d\Theta}{dX} \right) + \frac{1}{J}\rho_R R(X) = 0, \quad X \in (1, 2) \tag{77}$$

Since in 1-D $F_{11} = J$, (77) becomes:

$$\frac{d}{dX}\left(k_R \frac{1}{F_{11}}\frac{d\Theta}{dX} \right) + \rho_R R(X) = 0, \quad X \in (1, 2) \tag{78}$$

An illustrative figure of the coupled thermo-hyperelastic problem is depicted in Figure 2. Finally, the strain energy for this case is computed by (33)

$$\mathcal{U}(\Omega_0) = 3.779092061139837. \tag{79}$$

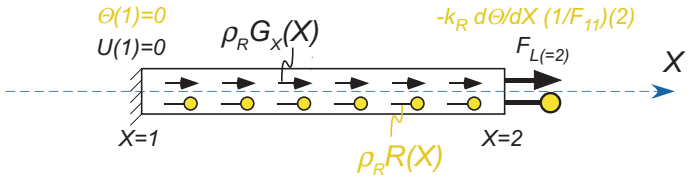

Figure 2: An illustration of the coupled problem of interest.

2.4.2 An exponential solution to the coupled thermo-hyperelastic problem with varying material properties

The material properties are taken to be functions of the temperature

$$\begin{aligned} \kappa(\Theta) &= \kappa_0 + \kappa_1\Theta + \kappa_2\Theta^2 = \frac{1}{2} + \Theta + \Theta^2, \\ c_{10}(\Theta) &= c_{10_0} + c_{10_1}\Theta + c_{10_2}\Theta^2 = \frac{3}{16} + \Theta + \frac{1}{2}\Theta^2 \\ k_R(\Theta) &= k_{R_0} + k_{R_1}\Theta + k_{R_2}\Theta^2 = 1 + \Theta + \frac{1}{10}\Theta^2 \end{aligned} \tag{80}$$

In addition the coefficient of thermal expansion is taken to be $\alpha_\Theta = 10^{-5}$.

The solution is taken to be

$$U(X) = X - e^{1-X} \quad \rightarrow J = 1 + U' = 2 + e^{1-X}, \quad F_{11} = 2 + e^{1-X} \tag{81}$$

$$\Theta(X) = X - e^{1-X} \tag{82}$$

Since the temperature Θ is to be understood as the difference compared to a reference stress-free temperature, we choose the reference temperature $\Theta_0 = 0$. The boundary conditions associated with the solution (81)-(82):
At $X = 1$, by substitution one obtains the Dirichlet BC:

$$U(1) = 0, \quad \Theta(1) = 0 \tag{83}$$

Two Neumann BCs are given for the coupled system at $X = 2$. Similar to the previous subsection, for the mechanical system the Neumann BC (first Piola-Kirchhoff stress tensor) at the right end $X = 2$ is given by:

$$F_L = F_{11}(X = 2)\tilde{T}_{XX}(X = 2) = 19.672325991 \tag{84}$$

The flux BC at $X = 2$ is:

$$q_n(X = 2) = -1.67441029811$$

$$
\begin{aligned}
\rho_R G_X \;=\; & e^{1-X}\left\{\frac{1}{10}\left[\frac{G_1^3}{\varphi_1^{15}}-\frac{\varphi_1^{15}}{G_1^7}\right]\left(\kappa_0+\kappa_1 G_2+\kappa_2 G_2^2\right)\right. \\
& -\frac{4}{3}\left(\frac{1}{G_1^2}-1\right)\frac{c_{10_0}+c_{10_1}G_2+c_{10_2}G_2^2}{G_1^{2/3}} \\
& +\frac{G_1^3}{10}\left(\kappa_0+\kappa_1 G_2+\kappa_2 G_2^2\right)\left(\frac{3e^{1-X}}{\varphi_1^{15}}+\frac{7e^{1-X}\varphi_1^{15}}{G_1^{10}}+\frac{15\alpha_\Theta G_3 G_1}{\varphi_1^{16}}+\frac{15\alpha_\Theta\varphi_1^{14}G_3}{G_1^9}\right) \\
& -\frac{aG_3}{5}\left(\kappa_1/2+a\kappa_2 G_2\right)\left(\frac{G_1^3}{\varphi_1^{15}}-\frac{\varphi_1^{15}}{G_1^7}\right)+\frac{8e^{1-X}}{3}\frac{c_{10_0}+c_{10_1}G_2+c_{10_2}G_2^2}{G_1^{11/3}} \\
& +\frac{4G_3}{3}\left(\frac{1}{G_1^2}-1\right)\frac{c_{10_1}+2c_{10_2}G_2}{G_1^{2/3}} \\
& \left.+\frac{8e^{1-X}}{9}\frac{c_{10_0}+c_{10_1}G_2+c_{10_2}G_2^2}{G_1^{5/3}}\left[\left(\frac{1}{e^{1-X}}+2\right)^2-1\right]\right\}
\end{aligned}
\tag{85}
$$

with

$$
\varphi_1 = 1+\alpha_\Theta\left(X-e^{1-X}\right),\quad G_3 = 1+e^{1-X},\quad G_2 = X-e^{1-X},\quad G_1 = e^{1-X}+2
$$

The distributed heat source is

$$
\rho_R R(X) = -\frac{1}{G_1^3}\left\{G_3^2 G_1\left(k_{R_1}+2k_{R_2}G_2\right)+e^{1-X}\left(k_{R_0}+k_{R_1}G_2+k_{R_2}G_2^2\right)\left(G_3-G_1\right)\right\} \tag{86}
$$

and the strain energy reads

$$
\mathcal{U}(\Omega_0) = 7.360556086526126594927128. \tag{87}
$$

2.4.3 A singular solution to the coupled thermo-hyperelastic problem with constant material properties

The material properties are taken to be

$$
\kappa = \frac{1}{2},\quad c_{10} = \frac{3}{16},\quad k_R = 1 \tag{88}
$$

In addition the coefficient of thermal expansion is $\alpha_\Theta = 10^{-5}$.

The solution is taken to be

$$
U(X) = (X-1)^{4/3} \qquad \rightarrow J = F_{11} = 1+U' = 1+\frac{4}{3}(X-1)^{1/3} \tag{89}
$$

$$
\Theta(X) = (X-1)^{4/3} \tag{90}
$$

Remark 2.2 *The second derivative of the displacement and the temperature is singular at $X = 1$. This example problem is being considered to evaluate the performance of the p-FEM for problems that are singular.*

Since the temperature Θ is to be understood as the difference compared to a reference stress-free temperature, we choose the reference temperature $\Theta_0 = 0$. The boundary conditions associated with the solution (89)-(90) at $X = 1$ are

$$U(1) = 0, \quad \Theta(1) = 0 \tag{91}$$

The Neumann BCs at $X = 2$ read

$$F_L = F_{11}(X = 2)\tilde{T}_{XX}(X = 2) = 1.75225076584, \quad q_n(X = 2) = -4/7 \tag{92}$$

nd the body force is

$$\rho_R G_X = \frac{16c_{10}G_2}{27G_1G_3^{2/3}}\left(\frac{1}{3} - \frac{2}{G_2G_3^2}\right) - \frac{4\kappa}{45G_1}\left(\frac{2G_3^3}{\varphi_1^{15}} + \frac{3\varphi_1^{15}}{G_3^7}\right) \tag{93}$$

with

$$\varphi_1 = 1+\alpha_\Theta\,(X-1)^{4/3}, \quad G_1 = (X-1)^{2/3}, \quad G_2 = \frac{1}{G_3^2}-1, \quad G_3 = \frac{4}{3}\,(X-1)^{1/3}+1.$$

The distributed heat source is

$$\rho_R R(X) = \frac{4k_R}{9G_1G_3}\left[\frac{4}{3}\,(X-1)^{1/3} - 1\right] \tag{94}$$

The strain energy for this case is computed by (33)

$$\mathcal{U}(\Omega_0) = 0.4996644085129540977. \tag{95}$$

3 Linearization and p-FE Implementation

We formulate here the numerical scheme, based on the p-version of the FE method, for the discretization of the weak forms. The two weak forms (65) and (66) are to be solved simultaneously. This leads to a coupled system of non-linear equations, which is solved using the Newton-Raphson method.

Assuming that the solution for a given state of loading and temperature boundary conditions is known, denote it by $U^{(k)}(X), \Theta^{(k)}(X)$, one can perform a linearization in the vicinity of that state, that yields the following system:

$$\mathcal{S}\Big(U^{(k)}(X), \Theta^{(k)}(X); V(X), \Upsilon(X)\Big) + D_U\mathcal{S} + D_\Theta\mathcal{S} \;=\; 0 \tag{96}$$

$$\mathcal{T}\Big(U^{(k)}(X), \Theta^{(k)}(X); V(X), \Upsilon(X)\Big) + D_U\mathcal{T} + D_\Theta\mathcal{T} \;=\; 0 \tag{97}$$

where

$$D_U\mathcal{S} \overset{\text{def}}{=} \frac{d}{d\alpha}\left[\mathcal{S}\left(U^{(k)}(X)+\alpha\Delta U,\Theta^{(k)}(X)+\beta\Delta\Theta;V(X),\Upsilon(X)\right)\right]_{\alpha=0,\beta=0} \tag{98}$$

$$D_\Theta\mathcal{S} \overset{\text{def}}{=} \frac{d}{d\beta}\left[\mathcal{S}\left(U^{(k)}(X)+\alpha\Delta U,\Theta^{(k)}(X)+\beta\Delta\Theta;V(X),\Upsilon(X)\right)\right]_{\alpha=0,\beta=0} \tag{99}$$

$$D_U\mathcal{T} \overset{\text{def}}{=} \frac{d}{d\alpha}\left[\mathcal{T}\left(U^{(k)}(X)+\alpha\Delta U,\Theta^{(k)}(X)+\beta\Delta\Theta;V(X),\Upsilon(X)\right)\right]_{\alpha=0,\beta=0} \tag{100}$$

$$D_\Theta\mathcal{T} \overset{\text{def}}{=} \frac{d}{d\beta}\left[\mathcal{T}\left(U^{(k)}(X)+\alpha\Delta U,\Theta^{(k)}(X)+\beta\Delta\Theta;V(X),\Upsilon(X)\right)\right]_{\alpha=0,\beta=0} \tag{101}$$

Remark 3.1 *The material properties $\kappa(\Theta), c_{10}(\Theta)$ and $k(\Theta)$ are explicit functions of the temperature, but we assume that α_Θ is a constant independent of the temperature. Otherwise, if α_Θ is temperature-dependent, the formulation may easily be adjusted.*

We define the following notations that are used in the linearization process:

$$J^{(k)} \overset{\text{def}}{=} 1+\left(U^{(k)}\right)' \tag{102}$$

$$\varphi^{(k)} \overset{\text{def}}{=} 1+\alpha_\Theta\left(\Theta^{(k)}-\Theta_0\right) \tag{103}$$

$$\tilde{T}^{(k)}_{XX} \overset{\text{def}}{=} \frac{\kappa(\Theta^{(k)})}{10}\left[\frac{(J^{(k)})^3}{(\varphi^{(k)})^{15}}-\frac{(\varphi^{(k)})^{15}}{(J^{(k)})^7}\right]+\frac{4c_{10}(\Theta^{(k)})}{3}(J^{(k)})^{-2/3}\left[1-(J^{(k)})^{-2}\right] \tag{104}$$

The index (k) defines the iteration index of the Newton-method. Detailed derivation of the various terms as a result of the linearization of the non-linear weak form are provided in Appendix A. Collecting all terms in Appendix A we finally obtain the

linearized explicit weak formulation for the coupled thermo-hyperelastic 1-D problem:

$$\begin{aligned}
&\int_{X_0}^{L}\left\{\frac{\kappa(\Theta^{(k)})}{10}\left(\frac{3(J^{(k)})^3}{(\varphi^{(k)})^{15}}+\frac{7(\varphi^{(k)})^{15}}{(J^{(k)})^7}\right)+\frac{8c_{10}(\Theta^{(k)})}{9}(J^{(k)})^{-2/3}\left[-1+4(J^{(k)})^{-2}\right]\right\}V'\,\Delta U'\,dX\\
+\;&\int_{X_0}^{L}\left(\tilde{T}_{XX}^{(k)}\right)V'\,\Delta U'\,dX+\int_{X_0}^{L}\frac{1}{10}\left.\frac{\partial\kappa(\Theta^{(k)}+\beta\Delta\Theta)}{\partial\beta}\right|_{\beta=0}\left(\frac{(J^{(k)})^4}{(\varphi^{(k)})^{15}}-\frac{(\varphi^{(k)})^{15}}{(J^{(k)})^6}\right)V'\,dX\\
-\;&\int_{X_0}^{L}\frac{3\kappa(\Theta^{(k)})}{2}\left(\frac{(J^{(k)})^4}{(\varphi^{(k)})^{16}}+\frac{(\varphi^{(k)})^{14}}{(J^{(k)})^6}\right)\alpha_\Theta V'\,\Delta\Theta\,dX\\
+\;&\frac{4}{3}\int_{X_0}^{L}\left.\frac{\partial c_{10}(\Theta^{(k)}+\beta\Delta\Theta)}{\partial\beta}\right|_{\beta=0}(J^{(k)})^{1/3}\left(1-(J^{(k)})^{-2}\right)V'\,dX\\
=\;&F_LV(L)+\int_{X_0}^{L}\rho_RG_XV\,dX-\int_{X_0}^{L}\tilde{T}_{XX}^{(k)}V'J^{(k)}\,dX
\end{aligned}\tag{105}$$

$$\begin{aligned}
&\int_{X_0}^{L}k(\Theta^{(k)})\,\Upsilon'\,\Delta\Theta'\,\frac{1}{J^{(k)}}\,dX+\int_{X_0}^{L}k(\Theta^{(k)})\;(\Theta^{(k)})'\,\Upsilon'\,\Delta U'\frac{1}{(J^{(k)})^2}\,dX\\
+\;&\int_{X_0}^{L}\left.\frac{dk(\Theta^{(k)}+\beta\Delta\Theta)}{d\beta}\right|_{\beta=0}(\Theta^{(k)})'\,\Upsilon'\frac{1}{J^{(k)}}\,dX\\
=\;&k(\Theta)\frac{d\Theta}{dX}\frac{1}{F_{11}}\Big|_L\,\Upsilon(L)+\int_{X_0}^{L}\rho_RR\Upsilon\,dX-\int_{X_0}^{L}k(\Theta^{(k)})\;(\Theta^{(k)})'\,\Upsilon'\frac{1}{J^{(k)}}\,dX
\end{aligned}\tag{106}$$

3.1 Discretization of the Coupled Thermo-Hyperelastic Weak Form by p-FEMs

The linearized thermo-hyperelastic weak form is discretized in this section by means of p-FEMs. Both ΔU and $\Delta\Theta$ have to be in H^1. Let us consider material properties $\kappa(\Theta)$, $c_{10}(\Theta)$ and $k_R(\Theta)$ that are quadratic functions in Θ, see Eqns.(80), then

$$\left.\frac{\partial\kappa(\Theta^{(k)}+\beta\Delta\Theta)}{\partial\beta}\right|_{\beta=0}=\left(\kappa_1+2\kappa_2\Theta^{(k)}\right)\Delta\Theta\tag{107}$$

$$\left.\frac{\partial c_{10}(\Theta^{(k)}+\beta\Delta\Theta)}{\partial\beta}\right|_{\beta=0}=\left(c_{10_1}+2c_{10_2}\Theta^{(k)}\right)\Delta\Theta\tag{108}$$

$$\left.\frac{dk_R(\Theta^{(k)}+\beta\Delta\Theta)}{d\beta}\right|_{\beta=0}=\left(k_{R_1}+2k_{R_2}\Theta^{(k)}\right)\Delta\Theta\tag{109}$$

hold.

3.1.1 Shape functions, mapping to the standard element & element matrices

The integral over the entire domain is split to a sum of integrals on elements. Each element $j = \left\{ X \middle| X_{j+1} < X < X_j \right\}$ is mapped to a standard element and the quantities of interest are represented as a linear combination of the shape functions (polynomials up to degree p) in the standard element.

$$X = \frac{1-\xi}{2} X_j + \frac{1+\xi}{2} X_{j+1}$$

For $p+1$ shape functions we use these based on the Legendre polynomials in Szabó and Babuška (1991).

$$\vec{N}^T = \{N_1(\xi),\ N_2(\xi),\ \cdots,\ N_{p+1}(\xi)\}$$

$$\begin{aligned} \Delta U(\xi) &= \vec{U}_\Delta^T \vec{N} && (110) \\ \Delta\Theta(\xi) &= \vec{\Theta}_\Delta^T \vec{N} && (111) \\ V(\xi) &= \vec{N}^T \vec{V} && (112) \\ \Upsilon(\xi) &= \vec{N}^T \vec{\Upsilon} && (113) \end{aligned}$$

A "combined" vector is constructed:

$$\vec{a}^T = \left\{ \vec{U}_\Delta^T,\ \vec{\Theta}_\Delta^T \right\} \tag{114}$$

with $\dim\vec{a} = 2(p+1)$. In this case the "tangent stiffness matrix" and "out of balance vector" associated with the coupled system (105)-(106) on the element level can be partitioned as follows:

$$\begin{bmatrix} K_{\mathcal{SS}} & K_{\mathcal{ST}} \\ K_{\mathcal{TS}} & K_{\mathcal{TT}} \end{bmatrix} \vec{a} = \begin{Bmatrix} \vec{r}_{\mathcal{S}} \\ \vec{r}_{\mathcal{T}} \end{Bmatrix} \tag{115}$$

After the mapping to the standard element and since $dX = \frac{\ell_m}{2} d\xi$ (ℓ_m is the length of element m) we have

$$(\Theta^{(k)})' = \frac{2}{\ell_m} \frac{d\Theta^{(k)}}{d\xi}$$

$$
\begin{aligned}
(K_{\mathcal{SS}})_{ij} &= \frac{2}{\ell_m}\int_{-1}^{1}\Bigg\{\Bigg[\frac{\kappa(\Theta^{(k)})}{10}\left(\frac{3(J^{(k)})^3}{(\varphi^{(k)})^{15}}+\frac{7(\varphi^{(k)})^{15}}{(J^{(k)})^7}\right)\\
&\qquad +\frac{8c_{10}(\Theta^{(k)})}{9}(J^{(k)})^{-2/3}\left(-1+4(J^{(k)})^{-2}\right)\Bigg]+\tilde{T}^{(k)}_{XX}\Bigg\}\frac{dN_i}{d\xi}\frac{dN_j}{d\xi}\,d\xi\\
(K_{\mathcal{ST}})_{ij} &= \int_{-1}^{1}\Bigg\{\frac{1}{10}\Big(\kappa_{R_1}+2\kappa_{R_2}\Theta^{(k)}\Big)\left(\frac{(J^{(k)})^4}{(\varphi^{(k)})^{15}}-\frac{(\varphi^{(k)})^{15}}{(J^{(k)})^6}\right)\\
&\qquad -\frac{3\kappa(\Theta^{(k)})}{2}\left(\frac{(J^{(k)})^4}{(\varphi^{(k)})^{16}}+\frac{(\varphi^{(k)})^{14}}{(J^{(k)})^6}\right)\alpha_\Theta\\
&\qquad +\frac{4}{3}\Big(c_{10R_1}+2c_{10R_2}\Theta^{(k)}\Big)(J^{(k)})^{1/3}\left(1-(J^{(k)})^{-2}\right)\Bigg\}\frac{dN_i}{d\xi}N_j\,d\xi\\
(K_{\mathcal{TS}})_{ij} &= -\left(\frac{2}{\ell_m}\right)^2\int_{-1}^{1}k(\Theta^{(k)})\,\frac{d\Theta^{(k)}}{d\xi}\,\frac{1}{(J^{(k)})^2}\,\frac{dN_i}{d\xi}\,\frac{dN_j}{d\xi}\,d\xi\\
(K_{\mathcal{TT}})_{ij} &= \frac{2}{\ell_m}\int_{-1}^{1}\Big(k_{R_1}+2k_{R_2}\Theta^{(k)}\Big)\frac{d\Theta^{(k)}}{d\xi}\,\frac{dN_i}{d\xi}\,N_j\,\frac{1}{J^{(k)}}\,d\xi+\frac{2}{\ell_m}\int_{-1}^{1}k_R(\Theta^{(k)})\,\frac{1}{J^{(k)}}\,\frac{dN_i}{d\xi}\,\frac{dN_j}{d\xi}\,d\xi\\
(r_{\mathcal{S}})_i &= F_L V(L)-\int_{-1}^{1}\tilde{T}^{(k)}_{XX}J^{(k)}\,\frac{dN_i}{d\xi}\,d\xi+\frac{\ell_m}{2}\int_{-1}^{1}\rho_R G_X(X(\xi))N_i\,d\xi\\
(r_{\mathcal{T}})_i &= k_R\frac{d\Theta}{dX}\frac{1}{F_{11}}\bigg|_L\Upsilon(L)-\frac{2}{\ell_m}\int_{-1}^{1}k_R(\Theta^{(k)})\,\frac{d\Theta^{(k)}}{d\xi}\,\frac{1}{J^{(k)}}\,\frac{dN_i}{d\xi}\,d\xi\\
&\qquad +\frac{\ell_m}{2}\int_{-1}^{1}\rho_R R(X(\xi))N_i\,d\xi
\end{aligned}
\tag{116}
$$

Remark 3.2 *The strong coupling of the two systems is manifested though the matrices $[K_{\mathcal{TS}}]$ and $[K_{\mathcal{ST}}]$ which are not zero.*

Remark 3.3 *One may observe that the tangent stiffness matrix is non-symmetric.*

Remark 3.4 *Both ΔU and $\Delta\Theta$ lay in the same FE space since both have to satisfy a 2^{nd} order elliptic ODE.*

The computation of the strain energy is performed by adding the contribution of the strain energy of each element. For each element, having the FE solution of the displacement and the temperature one computes the following:

$$U'(\xi)=\vec{a}^T_{Mech,\ell}\frac{d\vec{N}}{d\xi}\frac{d\xi}{dX}=\vec{a}^T_{Mech,\ell}\frac{d\vec{N}}{d\xi}\frac{2}{L^{(\ell)}}$$

$$\Theta(\xi)=\vec{a}^T_{\Theta,\ell}\vec{N},\quad\rightarrow\varphi(\xi)=1+\alpha_T(\Theta-\Theta_0)$$

$$J(\xi)=1+U',\quad J_M(\xi)=J/\varphi^3,\quad I_{\boldsymbol{C}_M}(\xi)=\frac{2+(1+U')^2)}{\varphi^3}$$

After having these for each element, then

$$\mathcal{U}_{FE} = \sum_{\ell} \int_{-1}^{1} c_{10R}(\Theta(\xi)) \left(I_{\boldsymbol{C}_M}(\xi)/J_M^{2/3} - 3 \right) + \frac{\kappa(\Theta(\xi))}{50} \left(J_M^5 + 1/J_M^5 - 2 \right) \frac{L^{(\ell)}}{2} d\xi$$

4 Numerical Examples

The problems for which an analytic solution was derived are being solved here by the p-FE methods presented. The numerical results are compared to the analytical solutions first for the uncoupled hyper-elastic problem, then for the coupled thermo-elastic problem with constant material coefficients, and we conclude by considering the coupled thermo-hyperelastic problem with material properties that change quadratically with the temperature.

Solid-mechanics part.

The example problems presented in section 2.2 are solved by a p-FE program implemented within *Matlab*. First the uncoupled solid mechanics problem is considered and the code is verified by comparing the FE results to the exact solutions in section 2.2. The FE results for the problem without body forces in section 2.2.1 converged immediately to the exact solution and are not shown herein.

The error in percentage between the FE and analytical solution is defined by:

$$Err(\%) \stackrel{\text{def}}{=} \frac{|U_{FE}(X) - U(X)|}{|U(X)|} \times 100 \tag{117}$$

The errors of the FE results for the three problems in sections 2.2.2-2.2.4 are presented in the graphs in Figure 3 for different p-levels of the FE solution. Also the number of load steps used, the number of elements in all example problems is 3 and the accumulated number of iterations are shown in the graphs. In all cases the Newton-Raphson convergence criterion was set to 10^{-10} relative error in consecutive solutions. The iterative procedure terminates if the relative error of each element of the out of balance vector is smaller than 10^{-10}. One may notice that the exact solution is fully recovered (up to roundoff error) when the polynomial degree of the FE space reaches that of the exact solution. It is worthwhile to mention that the bar of length 1 extends to a length of 2,6 and 14 (extreme stretch ratios) for the three problems shown in Figure 3. For the last case for example we applied the load in 10 steps, obtaining convergence within an accumulated around 70 iterations (seven iterations per load step on average).

Coupled system with constant material properties.

The coupled thermo-mechanical problem with constant material coefficients presented in section 2.4.1 is next solved. In this case both the displacement and the temperature are a polynomial of degree two. Using 3 equal elements and one load step, we increase the polynomial degree over the elements from 1 to 3, and use a tolerance of 10^{-10} as the relative error to terminate the Newton-Raphson iterations.

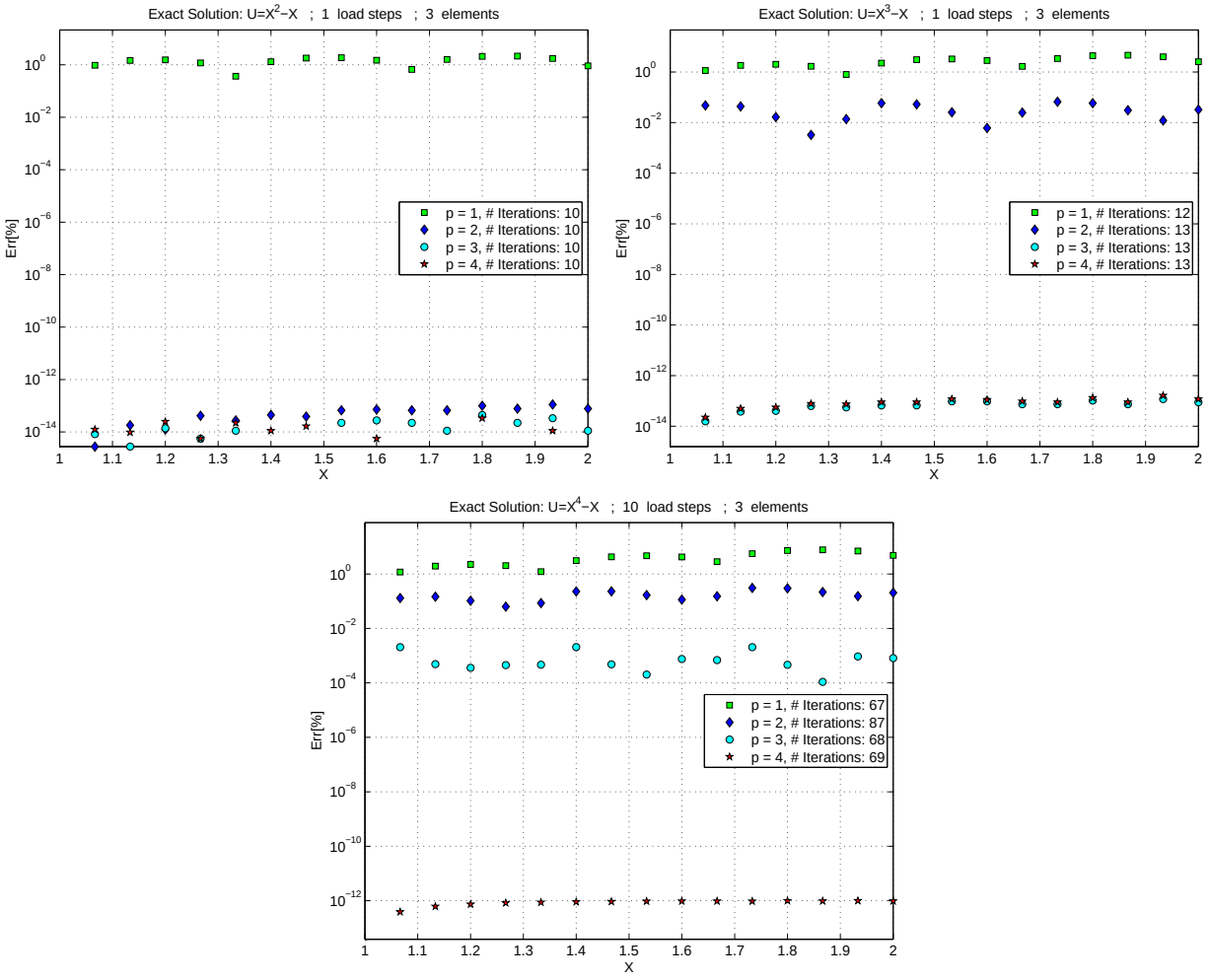

Figure 3: Solid mechanics problems and convergence.

A very fast convergence is obtained within 10 accumulated iterations. The error of the FE results is presented in the graphs in Figure 4 for the three different p-levels. As expected the exact solution is recovered at $p = 2$ for both the displacement and temperature.

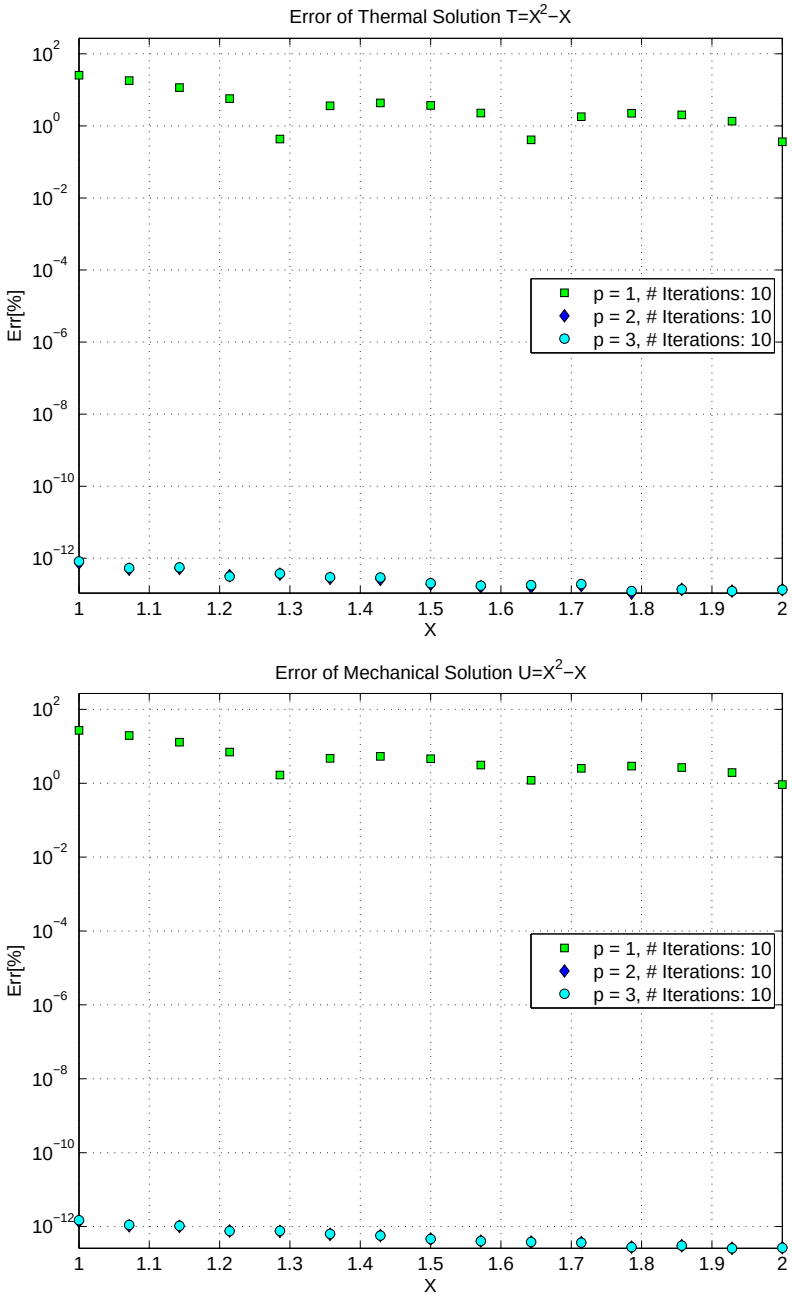

Figure 4: Coupled problem with constant material properties. Top - Convergence of temperature. Bottom - Convergence of displacement.

Coupled system with exponential solution and varying material properties.

The coupled thermo-mechanical problem with varying material coefficients presented in section 2.4.2 is next solved. In this case both the displacement and the temperature are smooth functions, therefore as the p-level is increased we expect an exponential convergence rate. Using 3 equal elements and five load steps, we increase the polynomial degree over the elements from 1 to 8, and use a tolerance of 10^{-10} as the relative error to terminate the Newton-Raphson iterations. A very fast convergence is obtained within 30 accumulated iterations. The error of the FE results is presented in the graphs in Figure 5 for the sequence of 8 polynomial-levels. The exponential convergence rate in energy norm, typical to the p-FEMs for linear problems, is demonstrated here. We define the relative error in energy norm (in percentage) by:

$$||e||_{\mathcal{U}}(\%) \stackrel{\text{def}}{=} \sqrt{\left|\frac{\mathcal{U}_{FE} - \mathcal{U}}{\mathcal{U}}\right|} \times 100 \tag{118}$$

Having computed the exact strain energy for this example problem in (87), we plot the error in energy norm versus the number of degrees of freedom for $p = 1, 2 \cdots, 6$ in Figure 6 (for $p \geq 7$ the error is less than $10^{-6}\%$ corresponding to an error of less than $10^{-12}\%$ in strain energy). For comparison we also present the convergence rate of the h-FEM with linear shape functions (keeping $p = 1$ or $p = 2$ on all elements and increasing the number of elements by a uniform mesh). The exponential convergence rate for the $p-$extension compared to the algebraic convergence rate of $h-$extension is clearly visible.

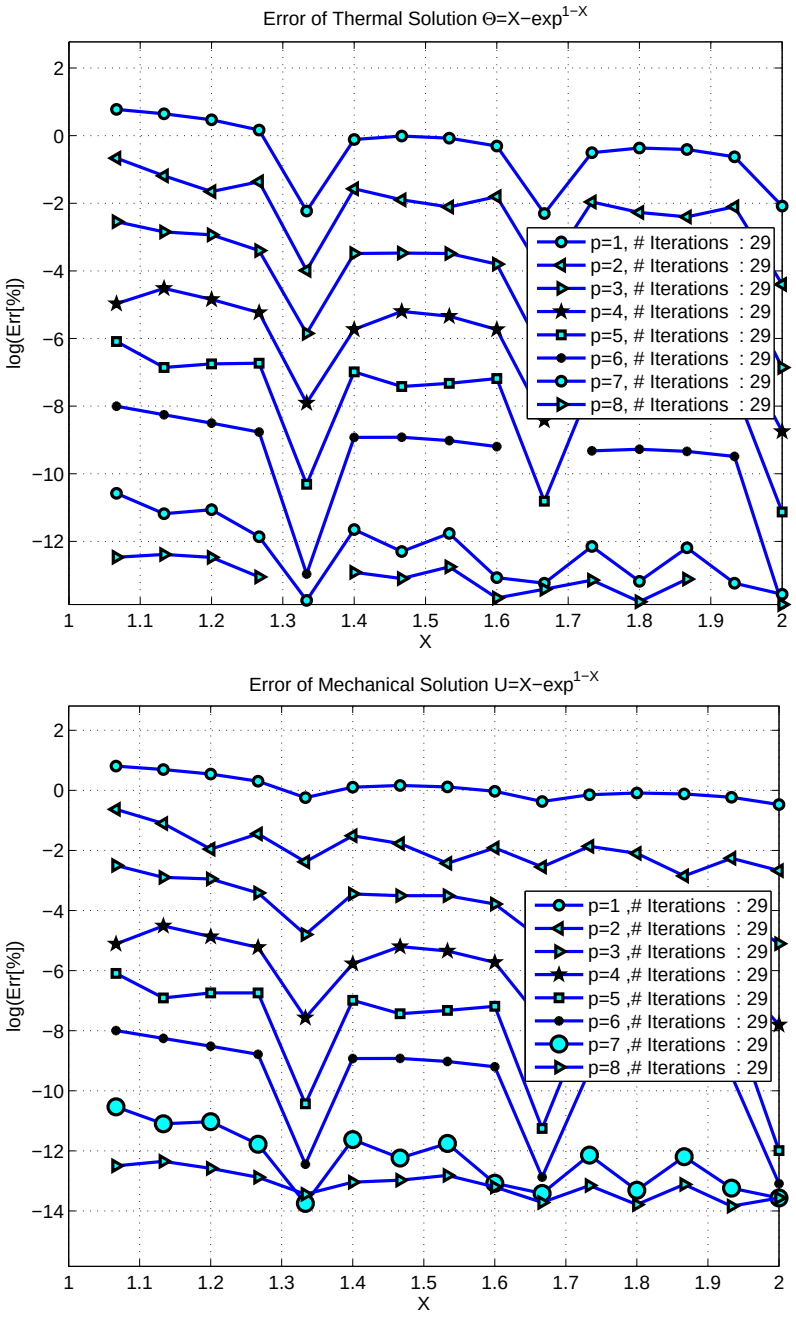

Figure 5: Coupled problem with varying material properties and exponential solution. Top - Convergence of temperature. Bottom - Convergence of displacement.

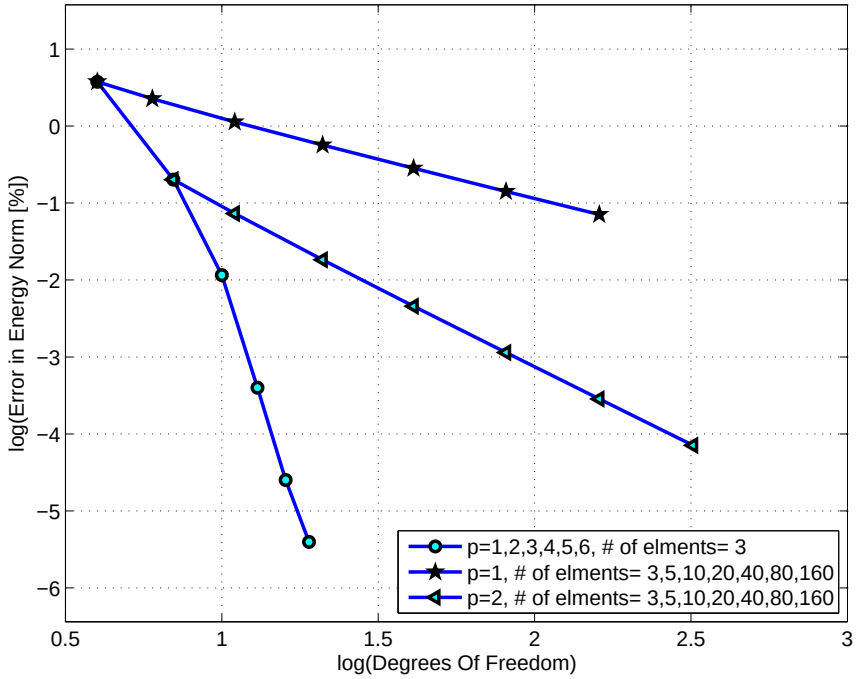

Figure 6: Convergence in energy norm $||e||_{\mathcal{U}}$ for the coupled problem with varying material properties and exponential solution: p- vs h-FEM.

Coupled system with a singular solution and constant material properties.

The coupled thermo-mechanical problem with constant material coefficients presented in section 2.4.3 has a singular solution, i.e. both the temperature and displacement second derivative is unbounded at $X = 1$. Therefore as the p-level is increased over a mesh consisting of elements equally distributed (no mesh refinement in the vicinity of the singular point $X = 1$) we expect an algebraic convergence rate (similar to the linear problem of elasticity), however, with a rate that is faster than the conventional h-version of the FEMs. Using 6 equal elements and one load step, we increase the polynomial degree over the elements from 1 to 8, and use a tolerance of 10^{-10} as the relative error to terminate the Newton-Raphson iterations. The stiffness matrix and load vector are integrated with a Gauss quadrature of order 54 to minimize the numerical integration error. A very fast convergence is obtained within 6 accumulated iterations. The error of the FE results is presented in the graphs in Figure 7 for the sequence of 8 polynomial-levels. One may clearly see the large numerical error concentrated in the first left element that has its node at the singular point.

The convergence rates in energy norm both for the p-FEM and h-FEM solutions, are demonstrated here. Using the exact strain energy for this example problem in (95), we plot the error in energy norm versus the number of degrees of freedom for $p = 1, 2 \cdots, 8$ in Figure 8 For comparison we also present the convergence rate of the h-FEM with parabolic shape functions (keeping $p = 2$ on all elements and increasing the number of elements by a uniform mesh). The faster algebraic convergence rate for the $p-$extension compared to the convergence rate of $h-$extension is clearly visible.

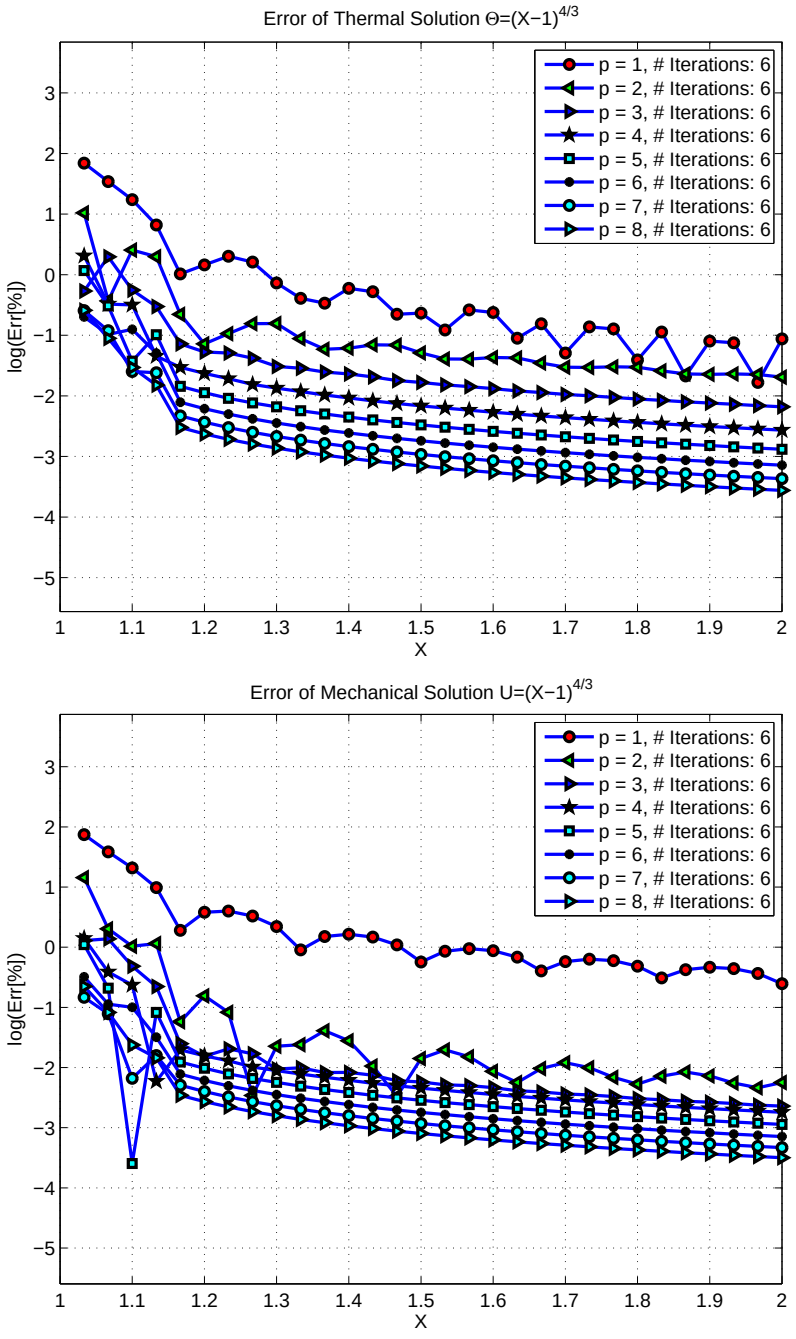

Figure 7: Coupled problem with constant material properties and singular solution. Top - Convergence of temperature. Bottom - Convergence of displacement.

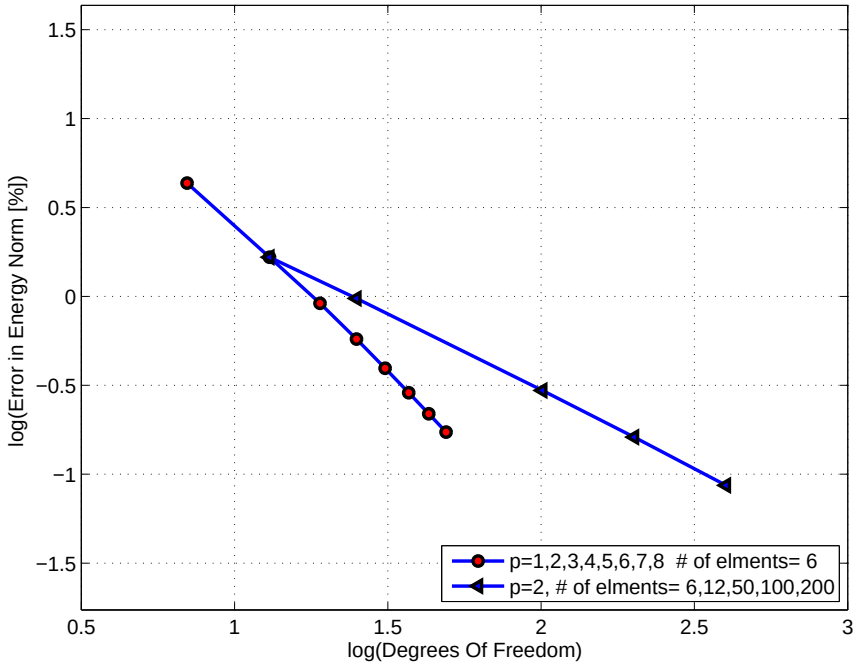

Figure 8: Convergence in energy norm $||e||_{\mathcal{U}}$ for the coupled problem with constant material properties and singular solution: p- vs h-FEM.

5 Summary and Conclusions

Thermo-hyperelastic two-way coupled problems under finite deformation with temperature dependent material properties are of major engineering importance. Such problems are realized in the tire industry (rubber under load and elevated temperatures) for example. To allow a transparent analysis and to develop high-order FE methods with demonstrated accuracy, a thermo-hyperelastic problem was formulated in an one-dimensional setting, for which several analytical solutions were computed. The weak-form for the coupled problems including temperature-dependent material properties (typically realized in reality) were also considered and the weak formulation was presented for such cases. The temperature dependence of the material properties resulted in a non-symmetric weak formulation.

High-order (p) monolithic finite element methods have been developed and their results were compared to several analytic solutions, demonstrating the extremely high accuracy at a very moderate number of degrees of freedom. The convergence properties of p-FEMs were investigated for coupled smooth solutions, as well as for solutions that contain singularities (second derivatives are unbounded at a point in the domain). Exponential convergence rates with respect to degrees of freedom were demonstrated for smooth coupled solutions whereas classical h-FE methods converge in an algebraic rate. For singular coupled solutions on uniform meshes an algebraic convergence rate is realized that is faster for p-FEMs compared to h-FEMs.

The numerical characteristics of p-FEMs applied to 1-D thermo-hyperelastic problems in a monolithic setting should be further investigated in the context of a realistic 3-D setting, including time-dependency. The results presented here provide the encouraging motivation in this direction. Evidence that similar characteristics may be expected in a 3-D setting is given in Erbts and Düster (2012). There implicit partitioned coupling schemes for same class of problems in 3-D, including time dependence, are discussed in the framework of p-FEMs, demonstrating encouraging results.

From the mathematical viewpoint the question of Hadamard's well-posedness for the coupled thermo-hyperelastic problem has to be yet investigated (the hyperelastic problem has been thoroughly investigated Ball (1977); Le Tallec (1994)). In this context, poly-convexity of the particular SEDF chosen has been addressed in Hartmann and Neff (2003). The coercivity of the nonlinear weak form, and especially the resulting linearized coupled system (105)-(106) has yet to be addressed.

In reality, the material properties cannot be measured precisely, and therefore are frequently provided with the uncertainties associated with their measurement. Therefore, the deterministic 1-D formulation presented here was a first step in an attempt to quantify the propagation of such material uncertainty through the coupled non-linear PDEs. $p-$FEMs for such stochastic ODE-system will be documented in a future publication.

Acknowledgments

The authors thank Mr. Hagen Wille (Technical University of Munich, Germany) for his help. The authors gratefully acknowledge the financial support of the German Research Foundation (DFG) under the grants RA 624/19-1 and HA 2024/7-2.

A Derivation of Terms Associated with the Linearization

Explicit terms in (98)-(101) are derived in this appendix.

The term $\mathcal{S}\Big(U^{(k)},\Theta^{(k)};V(X),\Upsilon(X)\Big)$:

Substituting (102)-(104) in (65) one obtains:

$$\mathcal{S}\Big(U^{(k)},\Theta^{(k)};V(X),\Upsilon(X)\Big)=\int_{X_0}^{L}\tilde{T}_{XX}^{(k)}V'J^{(k)}\,dX-\int_{X_0}^{L}\rho_R G_X V dX-F_L V(L) \quad (119)$$

The first part of "out of balance vector" is the result of (119).

The term $D_U\mathcal{S}$:

$$\begin{aligned} D_U\mathcal{S} &\overset{\text{def}}{=} D_U\left[\int_{X_0}^{L}\tilde{T}_{XX}\,V'J\,dX-\int_{X_0}^{L}\rho_R G_X V dX-F_L V(L)\right] \quad (120)\\ &=\int_{X_0}^{L}D_U\left[\tilde{T}_{XX}\right]\,V'J\,dX+\int_{X_0}^{L}\tilde{T}_{XX}\,D_U\left[V'J\right]\,dX \end{aligned}$$

Notice that $D_U\left[F_L V(L)\right]=0$ and $D_U\left[\int_{X_0}^{L}\rho_R G_X V dX\right]=0$ because the force F_L and the body force G_X are assumed to be independent of the deformation or the temperature field. For follower loads and temperature dependent BCs one would also need to take these into consideration in the linearization procedure.

Using (102) and (103) one observes that:

$$\begin{aligned} J(U^{(k)}(X)+\alpha\Delta U) &= J^{(k)}+\alpha\Delta U' \quad (121)\\ \varphi(\Theta^{(k)}(X)+\beta\Delta\Theta) &= \varphi^{(k)}+\beta\alpha_\Theta\Delta\Theta \quad (122) \end{aligned}$$

and using these we may compute $D_U\left[\tilde{T}_{XX}\right]$ in the first term of (120) according to (98) :

$$\begin{aligned} D_U\left[\tilde{T}_{XX}\right] &= \left\{\frac{\kappa(\Theta^{(k)})}{10}\left(\frac{3(J^{(k)})^2}{(\varphi^{(k)})^{15}}+\frac{7(\varphi^{(k)})^{15}}{(J^{(k)})^8}\right)\right. \quad (123)\\ &\quad\left.+\frac{8c_{10}(\Theta^{(k)})}{9}(J^{(k)})^{-5/3}\left[-1+4(J^{(k)})^{-2}\right]\right\}\Delta U' \end{aligned}$$

Similarly we may compute $D_U\left[V'J\right]=D_U\left[V'(1+U')\right]$ in the second term of (120):

$$D_U\left[V'J\right]=V'\Delta U' \quad (124)$$

We may now substitute (123) and (124) in (120) to obtain:

$$\begin{aligned} D_U\mathcal{S} &= \int_{X_0}^{L}\left\{\frac{\kappa(\Theta^{(k)})}{10}\left(\frac{3(J^{(k)})^2}{(\varphi^{(k)})^{15}}+\frac{7(\varphi^{(k)})^{15}}{(J^{(k)})^8}\right)\right. \\ &\quad \left.+\frac{8c_{10}(\Theta^{(k)})}{9}(J^{(k)})^{-5/3}\left[-1+4(J^{(k)})^{-2}\right]\right\}\Delta U'\,V'J^{(k)}\,dX \\ &+ \int_{X_0}^{L}\left(\tilde{T}_{XX}^{(k)}\right)V'\Delta U'\,dX \end{aligned} \tag{125}$$

The term $D_\Theta\mathcal{S}$:

Similarly to (120), one obtains:

$$D_\Theta\mathcal{S}=\int_{X_0}^{L}D_\Theta\left[\tilde{T}_{XX}\right]\,V'J\,dX+\int_{X_0}^{L}\tilde{T}_{XX}\,D_\Theta\left[V'J\right]\,dX \tag{126}$$

Here also $D_\Theta\left[T(L)AV(L)\right]=0$ because these are independent of the temperature, and furthermore $D_\Theta\left[V'J\right]=0$ because there is no explicit dependency of $V'J$ on Θ.

One obtains

$$\begin{aligned} D_\Theta\left[\tilde{T}_{XX}\right] &= \frac{1}{10}\frac{\partial\kappa(\Theta^{(k)}+\beta\Delta\Theta)}{\partial\beta}\bigg|_{\beta=0}\left(\frac{(J^{(k)})^3}{(\varphi^{(k)})^{15}}-\frac{(\varphi^{(k)})^{15}}{(J^{(k)})^7}\right) \\ &- \frac{3\kappa(\Theta^{(k)})}{2}\left(\frac{(J^{(k)})^3}{(\varphi^{(k)})^{16}}+\frac{(\varphi^{(k)})^{14}}{(J^{(k)})^7}\right)\alpha_\Theta\Delta\Theta \\ &+ \frac{4}{3}\frac{\partial c_{10}(\Theta^{(k)}+\beta\Delta\Theta)}{\partial\beta}\bigg|_{\beta=0}(J^{(k)})^{-2/3}\left(1-(J^{(k)})^{-2}\right) \end{aligned} \tag{127}$$

If κ and c_{10} are constants independent of Θ then (127) reduces to:

$$D_\Theta\left[\tilde{T}_{XX}\right]=-\frac{3\kappa}{2}\left(\frac{(J^{(k)})^3}{(\varphi^{(k)})^{16}}+\frac{(\varphi^{(k)})^{14}}{(J^{(k)})^7}\right)\alpha_\Theta\Delta\Theta \tag{128}$$

The term $\mathcal{T}\left(U^{(k)},\Theta^{(k)};V(X),\Upsilon(X)\right)$:

$$\begin{aligned} \mathcal{T}\left(U^{(k)},\Theta^{(k)};V(X),\Upsilon(X)\right) &= \int_{X_0}^{L}k(\Theta^{(k)})\;(\Theta^{(k)})'\,\Upsilon'\frac{1}{J^{(k)}}\,dX \\ &\quad -\int_{X_0}^{L}\rho_R R\Upsilon\,dX-k(\Theta)\frac{d\Theta}{dX}\frac{1}{F_{11}}\bigg|_L\Upsilon(L) \end{aligned} \tag{129}$$

The second part of "out of balance vector" is the result of (129).

The term $D_U\mathcal{T}$:

$$\begin{aligned} D_U\mathcal{T} &= D_U\left[\int_{X_0}^{L} k\,\Theta'\,\Upsilon'\frac{1}{J}\,dX - \int_{X_0}^{L}\rho_R R\Upsilon\,dX - k\frac{d\Theta}{dX}\frac{1}{F_{11}}\bigg|_L \Upsilon(L)\right] \\ &= \int_{X_0}^{L} k\,\Theta'\,\Upsilon' D_U\left[\frac{1}{J}\right]\,dX \\ &= -\int_{X_0}^{L} k(\Theta^{(k)})\;(\Theta^{(k)})'\,\Upsilon'\frac{\Delta U'}{(J^{(k)})^2}\,dX \end{aligned} \tag{130}$$

Here we assumed that $R(X)$ is independent of the deformation.

The term $D_\Theta\mathcal{T}$:

$$\begin{aligned} D_\Theta\mathcal{T} &= \int_{X_0}^{L} D_\Theta\left[k\right]\,\Theta'\,\Upsilon'\frac{1}{J}\,dX + \int_{X_0}^{L} k\,D_\Theta\left[\Theta'\right]\,\Upsilon'\frac{1}{J}\,dX \\ &= \int_{X_0}^{L}\frac{dk(\Theta^{(k)}+\beta\Delta\Theta)}{d\beta}\bigg|_{\beta=0}(\Theta^{(k)})'\,\Upsilon'\frac{1}{J^{(k)}}\,dX + \int_{X_0}^{L} k(\Theta^{(k)})\,\Delta\Theta'\,\Upsilon'\frac{1}{J^{(k)}}\,dX \end{aligned} \tag{131}$$

References

Armero, F., Simo, J. C., 1992. A new unconditionally stable fractional step method for non-linear coupled thermomechanical problems. Int. Jour. Numer. Meth. Engrg. 35, 737–766.

Ball, J. M., 1977. Convexity conditions and existence theorems in nonlinear elasticity. Archive for Rational Mechanics and Analysis 63 (4), 337–403.

Düster, A., Hartmann, S., Rank, E., 2003. p-FEM applied to finite isotropic hyperelastic bodies. Computer Meth. Appl. Mech. Engrg. 192, 5147–5166.

Ehlers, W., Eipper, G., 1998. The simple tension problem at large volumetric strains computed from finite hyperelastic material laws. Acta Mechanica 130, 17–27.

Erbts, P., Düster, A., 2012. Accelerated staggered coupling schemes for problems of thermoelasticity at finite strains. Comp. Math. with Appl. 64 (8), 2408–2430.

Hartmann, S., 2012. Comparison of the multiplicative decompositions $\boldsymbol{F} = \boldsymbol{F}_\Theta\boldsymbol{F}_M$ and $\boldsymbol{F} = \boldsymbol{F}_M\boldsymbol{F}_\Theta$ in finite strain thermo-elasticity. Technical Report Series Fac3-12-01, Faculty of Mathematics/Computer Sciences and Mechanical Engineering, Clausthal University of Technology (Germany).

Hartmann, S., Neff, P., 2003. Polyconvexity of generalized polynomial-type hyperelastic strain energy functions for near-incompressibility. Int. Jour. Solids and Structures 40 (11), 2767–2791.

Hartmann, S., Rothe, S., Frage, N., 2013. Electro-thermo-elastic simulation of graphite tools used in SPS processes. In: Altenbach, H. e. a. (Ed.), Generalized Continua as Models for Materials. Springer-Verlag, Berlin Heidelberg, pp. 143–161.

Heisserer, U., Hartmann, S., Düster, A., Yosibash, Z., 2008. On volumetric locking-free behavior of p-version finite elements under finite deformations. Communications Numer. Meth. Engrg. 24 (11), 1019–1032.

Le Tallec, P., 1994. Numerical Methods for Nonlinear Three-dimensional Elasticity. In: Ciarlet, P. G., Lions, J. L. (Eds.), Handbook of Numerical Analysis. Vol. 3. Elsevier, pp. 469–622.

Lu, S., Pister, K., 1975. Decomposition of deformation and representation of the free energy function for isotropic thermoelastic solids. Int. Jour. Solids Struc. 11, 927–934.

Netz, T., Düster, A., Hartmann, S., 2013. High-order finite elements compared to low-order mixed element formulations. Journal of Applied Mathematics and Mechanics 93, 163 – 176.

Szabó, B. A., Babuška, I., 1991. Finite Element Analysis. John Wiley & Sons, New York.

Yosibash, Z., Hartmann, S., Heisserer, U., Düster, A., Rank, E., Szanto, M., 2007. Axisymmetric pressure boundary loading for finite deformation analysis using p-FEM. Computer Meth. Appl. Mech. Engrg. 196, 1261–1277.

Yosibash, Z., Priel, E., 2011. p-FEMs for hyperelastic anisotropic nearly incompressible materials under finite deformations with applications to arteries simulation. Int. Jour. Numer. Meth. Engrg. 88, 1152–1174.